

THE EFFECT OF VENTILATOR CONFIGURATIONS IN NATURALLY VENTILATED GREENHOUSE APPLICATIONS

Sunita Kruger*, Leon Pretorius†

*University of Johannesburg, Kingsway Road, Auckland Park, Johannesburg, South Africa, skruger@uj.ac.za

†University of Johannesburg, Kingsway Road, Auckland Park, Johannesburg, South Africa, leonp@uj.ac.za

ABSTRACT

In this paper the climate inside a greenhouse subject to various vent configurations is investigated. The greenhouse considered is a four span glass greenhouse, containing a plastic partition separating the greenhouse into two compartments. The temperature and velocity distribution at plant level is numerically analyzed with computational fluid dynamics. Six cases were considered. The first three cases have the roof vents open to the leeward side, while the side ventilators are opened at 30° and 45° respectively, after which a second row of side ventilators opened at 45° were added to the geometry. The last three cases have the roof vents open towards the windward side, with the same side ventilator configuration as mentioned for the first three simulations. Contour plots for both temperature and velocity are discussed and analyzed. Results seem to indicate that the temperature and velocity at plant level are significantly influenced by the arrangement and number of vents. The presence of a plastic partition also has an effect on the climate. The temperature in the east span of the greenhouse is slightly higher for the leeward ventilators compared to the windward roof ventilators, and the temperature distribution is also less homogeneous if the roof ventilators are opened leeward. The velocity distribution in the west span for leeward roof ventilators are higher compared to windward ventilators, and also less homogeneous. Comparing the velocity distribution in the east span for both leeward and windward roof ventilators, the results show an increase in air movement for the east span of the greenhouse. It is also shown that CFD can be a useful tool in development and design of greenhouses.

INTRODUCTION

Natural ventilation is a popular means to ventilate the inside of greenhouses, which is of importance to control the indoor climate. The ventilation in naturally ventilated greenhouses is driven by pressure differences created at intentional openings, such as roof and side vents. These pressure differences are caused by temperature differences between the inside and the outside of the greenhouse, commonly known as the buoyancy or stack effect, as well as outside wind effect. (ASHRAE,2003). Greenhouses generally provide a protective environment for plants in order to typically produce horticultural crops out-of-season. In order to ensure the optimum production and quality of these crops, ventilation is vital to control air temperature, to renew carbon dioxide supply and to reduce the relative humidity of the greenhouse. As plants require carbon dioxide for photosynthesis, it is important that carbon dioxide be supplied continually; otherwise plant growth can be restricted. Controlling the indoor air temperature is of great importance, which is influenced by solar radiation (ASHRAE,2003). High temperatures inside the greenhouse are one of the causes leading to moisture stress. If the greenhouse temperature exceeds 32°C the plants may become severely stressed, as transpiration occurs at an elevated rate. This situation causes the plants to wilt, and hinders their growth. Extreme air movement may also cause plants to experience moisture stress, as the speed of the air causes high transpirational moisture loss. Certain fungus spores germinate only when the relative humidity is too high. Therefore ventilation generally aids in preventing plant disease. (Boodley, 1981)

Computational Fluid Dynamics is generally an advanced tool that can also be used for investigating the flow in and around a greenhouse structure. Recent advances in this field of CFD have increased the popularity of this method, and have been used in several studies to investigate the natural ventilation of various types of greenhouses. Mistriotis et al (1997) analyzed the efficiency of natural ventilation in single and multi-span greenhouses at low wind speeds. Various ventilator configurations were investigated using computational fluid dynamics. The models included realistic representations of heat sources and boundary conditions. The significance of roof and side-wall ventilators was confirmed using the results of this study (Mistriotis, 1997).

Airflows and temperature patterns through a single-span greenhouse with single and symmetrical roof ventilators were investigated by Boulard et al (1999). They found that for both single and two-sided roof ventilation, the airflow inside the greenhouse is characterized by a single convective cell. Although the presence of plants was ignored in the simulations, the results proved to be useful in improving greenhouse control and design. Kittas et al (2006) analyzed the microclimate and dehumidification effectiveness subject to different ventilator configurations. Heating and ventilation were investigated simultaneously for a tunnel greenhouse. It was concluded that the roll-up type vent configuration improved the dehumidification process, as the ratio of latent to sensible heat exchanged during the dehumidification process increased. In a study done by Ould Khaoua et al (2006), the ventilation efficiency of a greenhouse was analyzed by utilising CFD. The influence of wind speed and roof vent configuration on airflow and temperature patterns in a compartmentalised greenhouse was investigated. They found that the ventilation rate efficiency was considerably increased by orientating the roof vents windward. The effect of vent arrangement on windward ventilation of a tunnel greenhouse was investigated by Barzanas et al (2004). The results indicated that for evaluating the performance of various ventilation systems, the best criterion is not necessarily the highest obtainable ventilation rate. Other criteria that should be taken into consideration as well are air velocities and corresponding aerodynamic resistance in the region covered by the crop and air temperature differences between the inside and outside of the greenhouse. These criteria led to the conclusion that a combination of roof and side openings provides an appropriate solution for ventilation.

The objective of the current study is to investigate the influence of different combinations of side and roof ventilators on the indoor climate of a fourspan greenhouse. The first greenhouse geometry was evaluated against experimental results found in the literature (Ould Khaoua, 2006; Kruger,2007). The effect of adding a second row of side ventilators is also investigated.

COMPUTATIONAL FLUID DYNAMICS

Fundamental Equations

In computational fluid dynamics (CFD), transport equations generally describe the mechanics of both solid and fluid continua. The transport equations are derived assuming that mass, momentum and energy are conserved within the continuum. (StarCCM+,2006). The commercial CFD software Star-CCM+ was used to simulate the atmosphere inside the greenhouse of the current study, which is based on the finite volume method. This method subdivides the solution domain into a finite number of small control volumes, which correspond to the cells of a computational grid. Discrete versions of the integral form of the continuum transport equations are applied to each volume. The objective of this method is to obtain a set of linear algebraic equations to solve. An

algebraic multigrid solver is then used to solve the resulting linear equations. To illustrate this, the transport of a simple scalar will be considered. The continuous integral form of the governing equation is typically given by Eq. (1), (StarCCM+, 2006):

$$\frac{d}{dt} \int_V \rho \phi dV + \oint_A \rho \phi (\mathbf{v} - \mathbf{v}_g) \cdot d\mathbf{a} = \oint_A \Gamma \nabla \phi \cdot d\mathbf{a} + \int_V S_\phi dV \quad (1)$$

The four terms in the above equation are the transient term, the convective flux, the diffuse flux and the volumetric source term respectively. The transient term is generally only included where time effects become dominant. Each term is formulated mathematically in the StarCCM+ documentation (2006), as well as in for instance Versteeg et al (2007). If the continuous integral form of the governing equation is discretized, Eq. (2) is obtained:

$$\frac{d}{dt} (\rho \phi V)_0 + \sum_f [\rho \phi (\bar{\mathbf{v}} \cdot \bar{\mathbf{a}} - G)]_f = \sum_f (\Gamma \nabla \phi \cdot \bar{\mathbf{a}})_f + (S_\phi V)_0 \quad (2)$$

The discretization procedure is described in some detail by Patankar (1980) and Versteeg (2007). In order to model natural convection, the buoyancy source terms are included in the momentum equation by activating the gravity model. By selecting the constant density flow option, the buoyancy source term can be approximated by implementing the Boussinesq model as shown below in Eq. (3):

$$f_g = \rho \bar{g} \beta (T_{ref} - T) \quad (3)$$

StarCCM+ contains two models to model flow and energy, namely the segregated and coupled flow models. In order to solve the conservation equations for mass, momentum and energy simultaneously using a time or pseudo-time marching approach, the coupled flow model was chosen as well an extension of this model, the coupled energy equation. The formulation used by this model is particularly robust for solving flows with dominant source terms such as buoyancy. (StarCCM+, 2006) The turbulent nature of inner and outer flows in greenhouses were already indicated by previous investigations (Boulard et al, 2000) In StarCCM+ turbulence is also simulated by solving the Reynolds-averaged governing equations for momentum, energy and scalar transport. Various turbulence models are available in StarCCM+; for this investigation the standard $k-\epsilon$ model was implemented. This model is a two-equation model in which transport equations are solved for the turbulent kinetic energy k and its dissipation rate ϵ . The transport equations used are in the form suggested by Jones and Launder (1971). Additional terms have been added in StarCCM+ to account for buoyancy (in this case the Boussinesq approximation) and compressibility effects.

Description of the Numerical Greenhouse Model

The greenhouse investigated in this paper is approximated from the data in an investigation by Ould Khaoua et al (2006). It represents a fourspan greenhouse (width, 4 by 9.60m; length, 68m; eaves height, 3.90m; ridge height, 5.9m) covered with 4mm thick horticultural glass, containing a central plastic partition (Figure 1). Each span has continuous roof vents. The length of the shelves and width of the ventilator openings were approximated from the data in Ould Khaoua (2006).

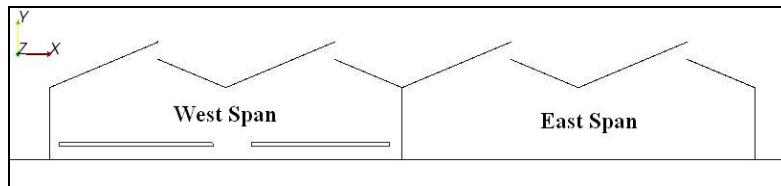


Figure 1: *Fourspan Greenhouse with plastic partition (Roof Vents Open Leeward)*

Ornamental plants were present inside the greenhouse during the experiments conducted by Ould Khaoua et al (2006). The height of the plants was 0.2m, while the shelves containing the plants were 0.75m. The presence of the young plants was ignored however, since they had a small size and a low transpiration rate. The gravitational constant was chosen to act in the negative y-direction, and the wind was acting in an easterly

direction perpendicular to the greenhouse, with a velocity of 1 m/s. The boundary conditions imposed on the model are shown in table 1.

Table 1: *Boundary Conditions used in CFD Model Similar to Ould Khaoua (2006)*

PARAMETERS	VALUES
Inlet Air	
Velocity at 6m [m/s]	1.4
Temperature [°C]	22.2
Temperature [°C]	
Outside Air	22.2
Outside Ground	27.9
Inside Ground	27.3
Roof	33.6
Plastic Central Partition	31.3
Glass Walls	29.1

A large rectangular control volume was constructed around the greenhouse in order to minimize interference with the flow in the immediate vicinity of the greenhouse. The height measured 160m, while the outflow was defined far downstream. The entire length of the control volume measured 334m. The solution domain was meshed using a polyhedral meshing model (Starccm+,2006). A tetrahedral mesh was created initially, after which a special dualization scheme was implemented to generate the polyhedral mesh, which consists of arbitrary shaped polyhedral cells. A brick-shaped volume shape was used to refine the mesh in and around the greenhouse, defined with a size relative to the base size of the core mesh. After careful consideration, it was decided to refine the mesh to 5% of the base size. The refined mesh is shown in Figure 2.

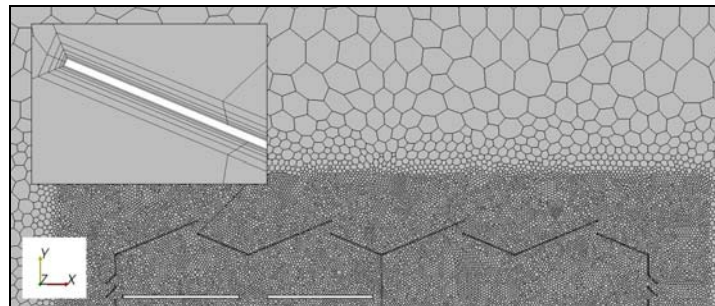


Figure 2: *Refined Mesh around the Greenhouse*

The prism layer meshing model was activated during the meshing process to ensure appropriate modelling of the turbulence in the boundary layer. The prism layer mesh consisted of 5 orthogonal prismatic cells, with a combined thickness of 0.01m. The prism layer was present on all the wall-type boundaries in the solution domain. The prism layer is shown in the enlarged area of Figure 2. The top part of the computational domain was initially defined as a symmetry plane. To reduce running time, the three-dimensional mesh was converted to a two-dimensional mesh. The final mesh consisted of approximately 30 238 cells.

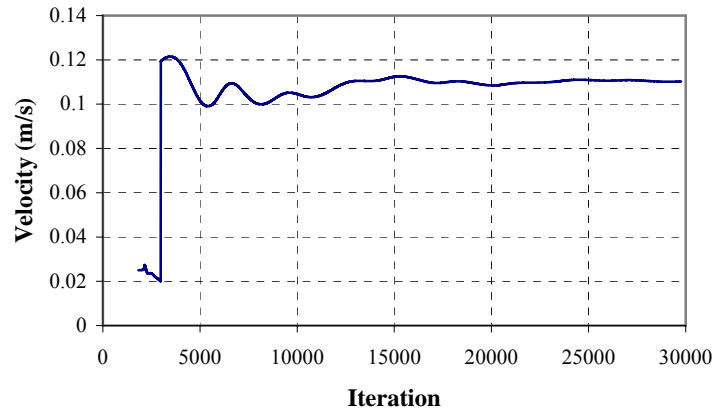


Figure 3: Variation of velocity with iteration (Monitoring Point)

As an initial solution, steady, laminar conditions were assumed, after which the turbulence model was activated. The results indicated poor convergence, as well as an inherently transient flow. Lastly, the coupled solver was activated together with gravity and the implicit unsteady solver used in StarCCM+ (2006). Figure 3 is a plot of a point monitoring the flow inside the greenhouse during the unsteady flow simulation for a typical case. It should be clear from the graph that the flow is intrinsically unsteady. It was therefore decided to use the results for each simulation at a certain point in time where the monitor point seemed to be reasonably converged to a steady state.

Ventilator Configurations used for Simulations

The following configurations of roof and side vents were used to investigate the climate inside the greenhouse:

- 1) Roof Vents open Leeward
 - a. Side vents open at angle of 45°
 - b. Side vents open at angle of 30°
 - c. Double row of side vents open at angle of 45°
- 2) Roof Vents open Windward
 - a. Side vents open at angle of 45°
 - b. Side vents open at angle of 30°
 - c. Double row of side vents open at angle of 45°

These configurations were specifically decided on to assess the effect of number of vents and opening size on the indoor greenhouse climate. As such a parametric study can be done for design purposes of greenhouses, the results of for instance the 45 degree opening can in future be assessed against the results obtained by Bartzanas et al (2004).

RESULTS

The initial closed greenhouse containing only roof vents was previously evaluated to some extent by Kruger et al (2007). The model was then adapted to contain variations of side and roof ventilators.

Roof Vents Open Leeward

For the first simulations, the side vents were opened only 30 degrees. Figure 4 shows a scalar plot of the velocity and temperature contours for this case. The flow for this configurations is characterized by a strong flow of current moving upwards immediately towards and out the first roof vent, while part of the flow forms a clockwise cell circulating above the first shelf. At the second roof vent, air is sucked in, creating a second counter clockwise cell. Air is sucked in at the back vent, also moving upwards toward the roof vent. Most of the flow in this stream forms a counter clockwise cell, while a small part moves out the last roof vent. In the third compartment, a weaker cell is formed from part of the flow from the cell in the last compartment. Most of this

flow moves out the third roof vent, while a counter clockwise cell is circulating close to the plastic partition. The temperature plot indicates that the climate inside the greenhouse is warmer compared to outside, with a more significant rise in temperature from about 297K to approximately 301K next to the plastic partition in the west span (third compartment), coinciding with the convective cell.

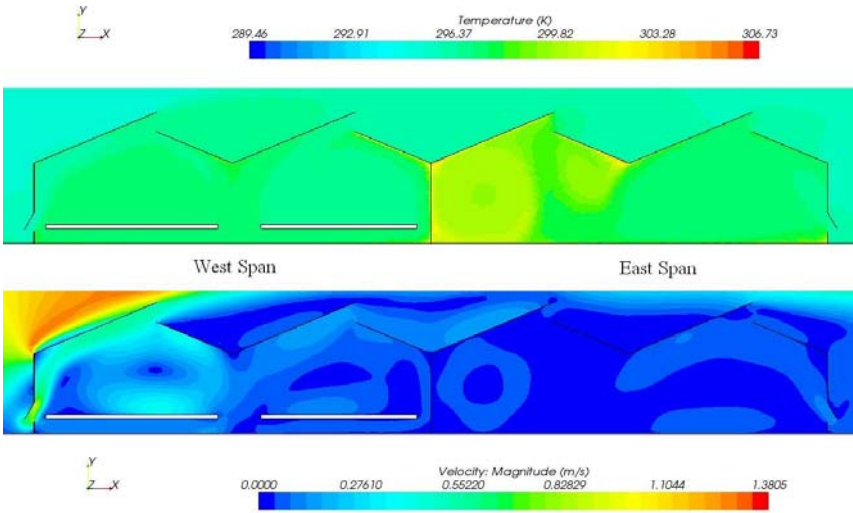


Figure 4: Velocity and Temperature Contour Plot (Side Vents 30°, Roof Vents open Leeward)

Secondly, the openings of the side vents were increased to an angle of 45 degrees. Figure 5 shows a contour plot of the temperature distribution at the top with the velocity distribution within the greenhouse at the bottom.

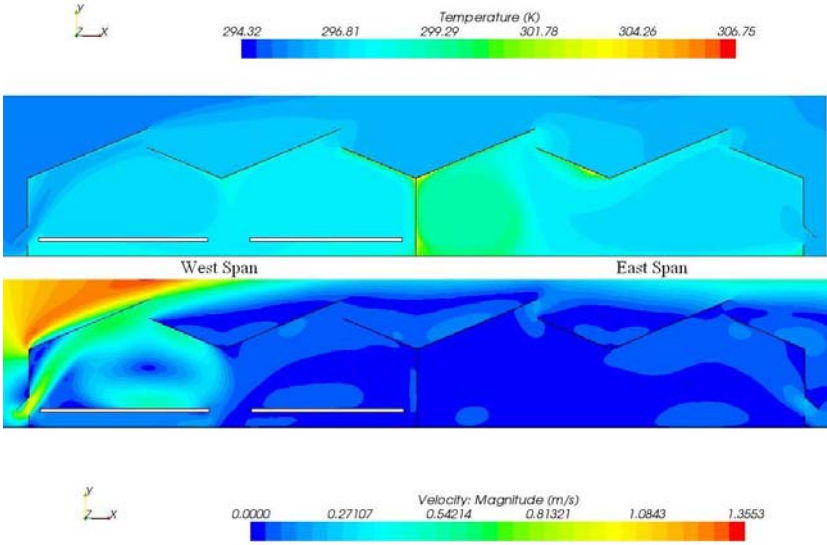


Figure 5: Velocity and Temperature Contour Plot (Side Vents 45°, Roof Vents Open Leeward)

Figure 5 indicates a slightly stronger current of air entering the greenhouse from outside, and is forced towards and out the first roof vent. Part of this air stream creates a clockwise rotating cell in the first compartment of the greenhouse. A clockwise cell is formed on the roof outside between the second and third compartments, forcing air to enter the greenhouse at the second roof vent. The second counter clockwise cell in the west span is much weaker compared to the first cell. Air is also sucked in at the back of the greenhouse through the side vent, moving out and towards the last roof vent, and creating a counter clockwise rotating cell. Part of this flow follows the contour of the roof, moving out the third roof vent. A smaller counter clockwise cell is formed next to the plastic partition. The temperature rise next to the plastic partition in the east span is slightly less (approximately 2°C) compared to the previous rise of 4°C.

To investigate an alternative possibility of improving the indoor climate, a second row of side vents opened at an angle of 45 degrees was added to the front and back glass walls of the greenhouse. The velocity and temperature contour plots are shown in Figure 6.

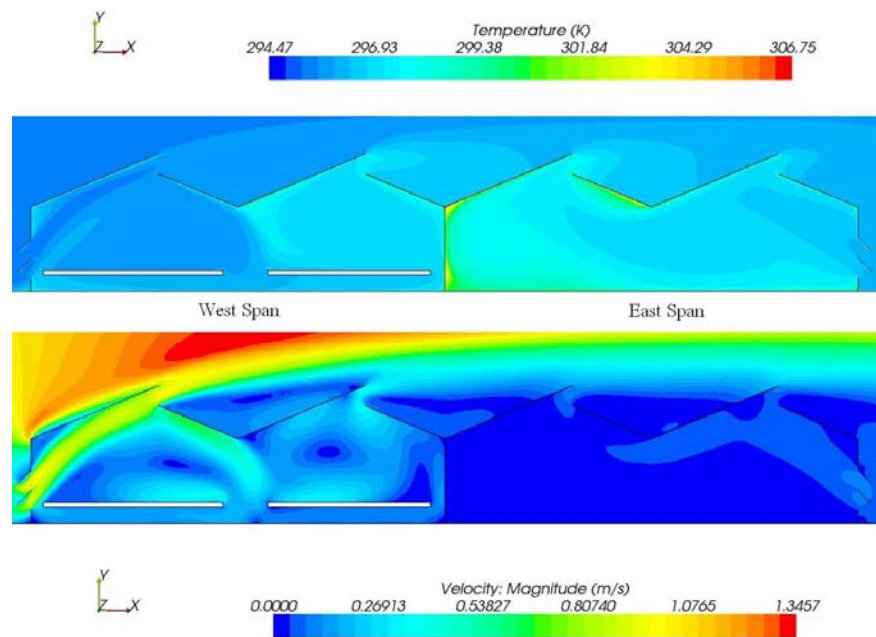


Figure 6: *Velocity and Temperature Contour Plots (Double Side Vents 45°, Roof vents open Leeward)*

From the contour plot in Figure 6 it can be seen that flow is still characterized by a strong current of air moving through the front side vents, and immediately progressing toward the roof. Most of the flow proceeds through the first roof ventilator, while some of the flow once again forms clockwise rotating cell. The flow then splits, as some of the flow moves over the first shelf, and the rest moves in opposite directions underneath the shelves. A small part of the first cell creates a second counter clockwise cell in the second compartment and some of the flow from this cell is forced out the second roof vent. Air is sucked at the back two side vents, and rises toward the last roof ventilator, where a portion of the flow exits. The rest of the flow proceeds toward and out the third roof ventilator. The velocity contour plot illustrates that there is little movement (average velocity of 0.017m/s) in the last two compartments compared to the first two.

Figure 7 compares the air velocities at a height of 1m inside the entire greenhouse for all three configurations with a leeward roof ventilator. The wind enters the greenhouse with the highest velocity for the configuration containing two side vents, and the vents opened at 30 degrees had lowest entrance velocity. Where the roof vents are open 45 degrees, the air moves with a velocity of approximately 0.46 m/s towards the first roof vent, whereas both the 30 degree and double configurations have an approximate velocity of 0.35 m/s. Only the double roof vent configuration has quite a high velocity above the second shelf, whereas all the configurations have relatively low movement in the east span. It has been reported by Wadsworth, Morse and Evans in a study done by Kitaya et al (2004) that the optimum air velocities for plant growth varies between and 0.3 and 0.7 m/s. Therefore it is clear that the ventilation in the east span of the greenhouse might not be sufficient for optimum plant production as the velocity distribution is lower than 0.1 m/s for the two last spans due to the presence of the full plastic partition.

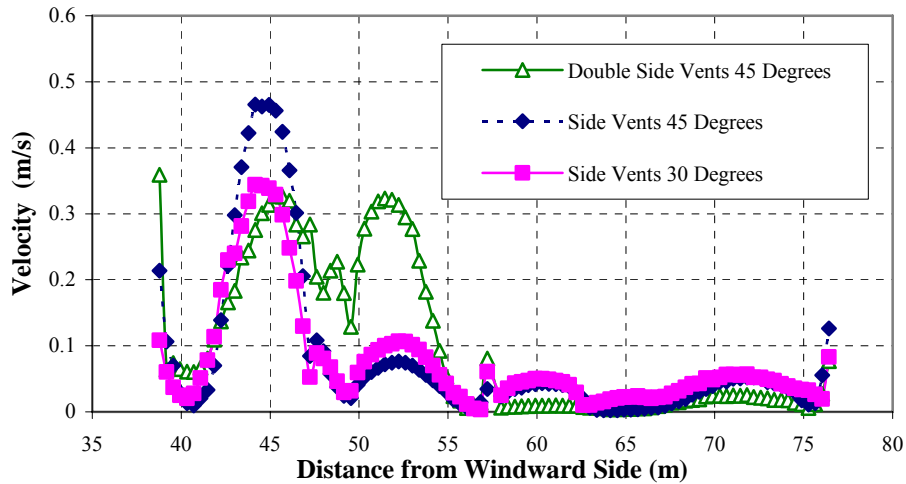


Figure 7: Comparison of Velocities inside Greenhouse (Roof Vents open Leeward)

A comparison of the temperature distributions within the greenhouse for each configuration with leeward opened roof vents is shown in Figure 8.

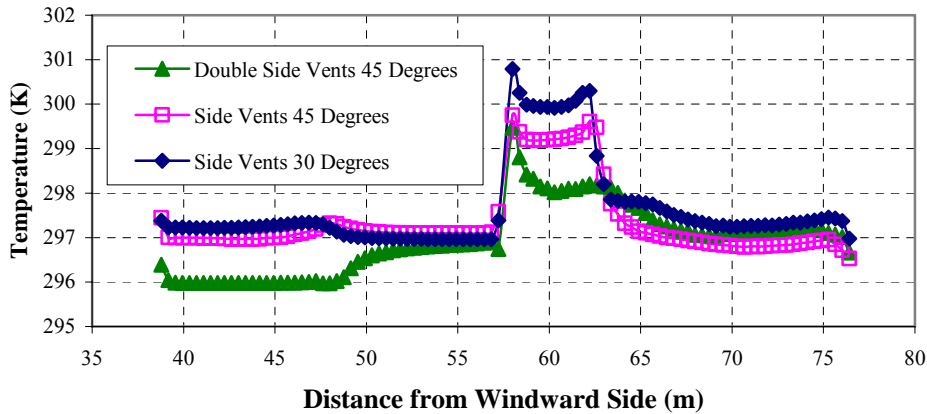


Figure 8: Comparison of Temperature Distributions for Different Configurations (Roof Vents open Leeward)

The temperature inside the first east span (first two spans) is relatively homogeneous for all three cases, but in the west span a cell of warm air circulates close to the plastic partition. The temperature in this region is approximately between 2 and 4.3 degrees C above to the rest of the greenhouse. Clearly when the side vents are opened at the smallest angle, the temperature in the front compartment is the highest, as well as in the third compartment next to the plastic partition. The single row ventilators yields a similar temperature distribution in the west spans, as well as the two east spans, except for a small drop in temperature (approximately 2°C) in the third compartment. As far as homogeneity is concerned, the double side ventilators seem to have a more uneven temperature distribution compared to the single side ventilators in the front two compartments. For the last two compartments it seems as if the double ventilators provide a more homogeneous temperature distribution compared to the single side ventilators. This is visible in the various temperature contour plots.

Roof Vents Open Windward

For the second set of simulations, the roof ventilators were orientated windward. In the first case the sidewall ventilators were opened once again at an angle of 30 degrees. Figure 9 illustrates the velocity and temperature contour plot for this configuration.

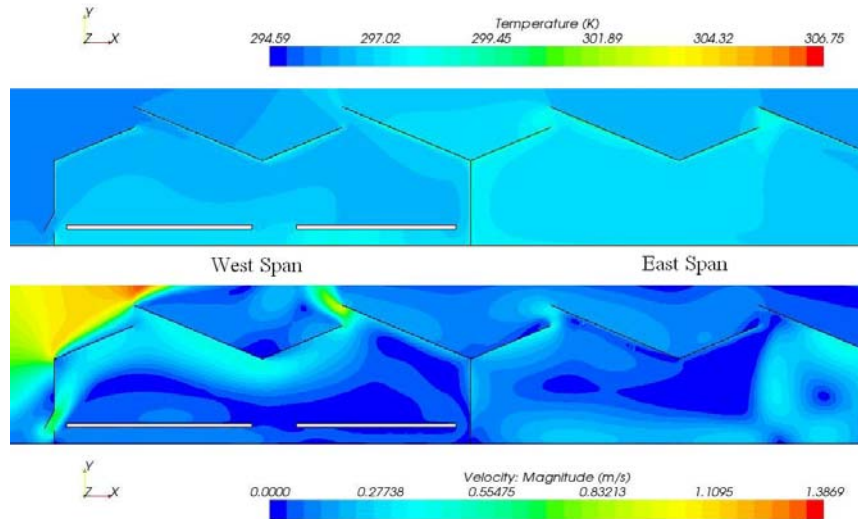


Figure 9: Temperature and Velocity Contour Plot (Side Vents 30°, Roof Vents open Windward)

The flow in the first two compartments is characterized by a strong air current entering the side ventilator, moving up towards the roof, where it is joined by a second air stream entering through the first roof ventilator. Most of this combined air stream follows the contour of the roof; where it exits at the second roof vent, and a small portion creates a clockwise rotating cell above the first shelf. In the second compartment next to the plastic partition there is relatively little movement above the second shelf. A strong air current of about 0.3 m/s enters through the back side ventilator as well, and moves up towards the roof immediately. A strong counter clockwise cell is created, with some air separating close to the ground, where it continues to move along the greenhouse floor toward the plastic partition. The flow is forced up against the plastic partition, and out the third roof ventilator, while a clockwise cell is formed. A very small portion of the flow moves back into the greenhouse along the roof and exits at the fourth roof ventilator.

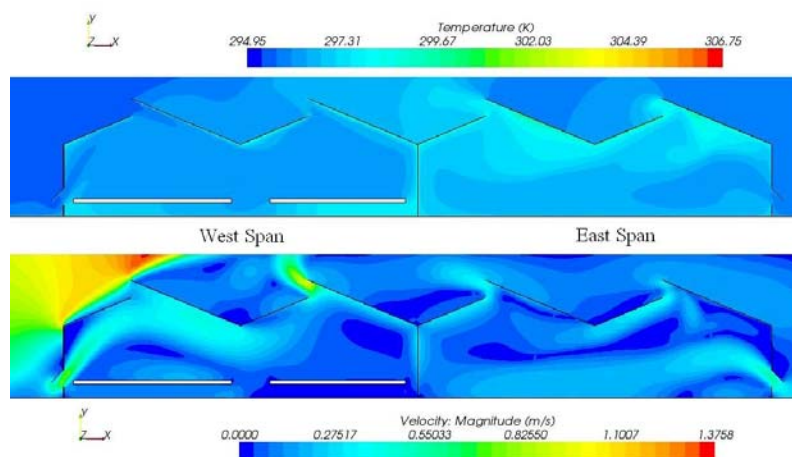


Figure 10: Temperature and Velocity contour Plot (Side Vents 45°, Roof Vents open Windward)

In the case of a 45° side ventilator opening (Figure 10), the air entering the side vents (approximately 0.5 m/s) is joined by a second air stream entering through the first roof ventilator. The joined air stream moves downward, following the contour of the roof, and splits up above the space between the shelves. Part of the flow moves toward the right, and creates a clockwise cell above the first shelf, while the rest moves underneath the shelf. The other part moves over the second shelf, up against the plastic partition and toward and out the second roof vent. The air entering at the back of the greenhouse creates a small counter clockwise vortex right underneath the side vent along the floor, while the main part forms a flow of air that moves down to the floor. This air stream moves along the floor, and up against the plastic partition. Most of the air exits through the third roof vent, while a small portion remains inside the greenhouse, and moves out the fourth roof ventilator. From

the temperature plot it can be seen that the air is cooled at the floor level, but areas with low air movement, such as close to the roof, corresponds to slightly higher temperatures.

Lastly, a second row of side ventilators was added once again. The temperature and velocity contour plots for this case can be seen in Figure 11.

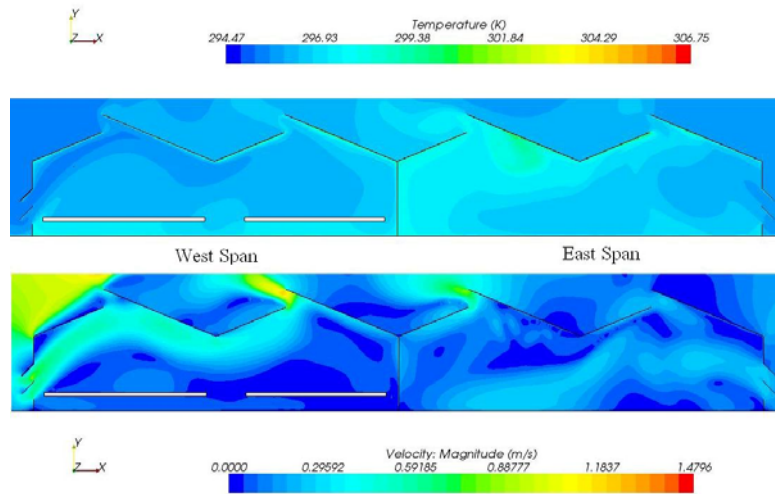


Figure 11: *Temperature and Velocity Contour Plots (Double Side Vents 45°, Roof Vents open Windward)*

In this case, the flow moves through the side ventilators at a relatively high speed, and then proceeds toward the roof. Only a small portion moves out the first roof vent, while the largest portion of the flow moves downward against the inside of the roof. A clockwise cell is formed above the first shelf, but most of the flow moves out the second roof vent. The bottom part of this fluid stream forms two weaker clockwise and counter clockwise cells. Part of the second cell moves close to the roof towards and out the second roof ventilator. The flow in the last two compartments is defined by a series of rotating cells. The air is sucked in through the back vents, firstly forming a small counter clockwise cell before falling the floor. The flow then moves along the floor towards the plastic partition, upward and out the third roof ventilator. Air is also sucked in at the fourth roof ventilator, which joins the main air stream below the roof.

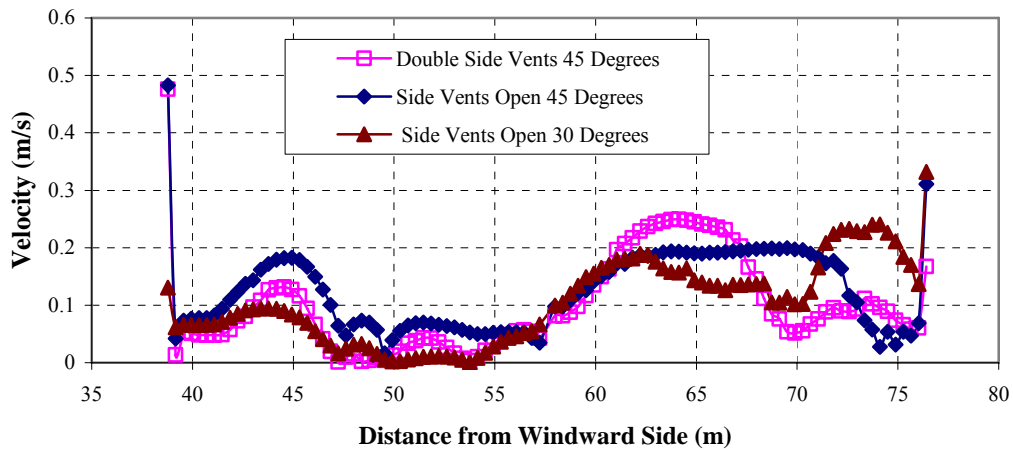


Figure 12: *Comparison of Velocities for all three vent configurations (Roof vents open Windward)*

Figure 12 is a comparison of the velocity distributions at plant level (1m) for all three configurations throughout the greenhouse with windward roof ventilators. For all three configurations, the velocity varies quite significantly throughout. The maximum velocity (approximately 0.25 m/s) occurs in the third compartment when a row of double side ventilators are opened. Changing the opening from 30° to 45° has a noticeable influence on the climate inside. Velocities inside the last two spans are relatively higher overall compared to the first two spans. The high velocities of both the front and the back air streams moving through the side vents are also clearly visible.

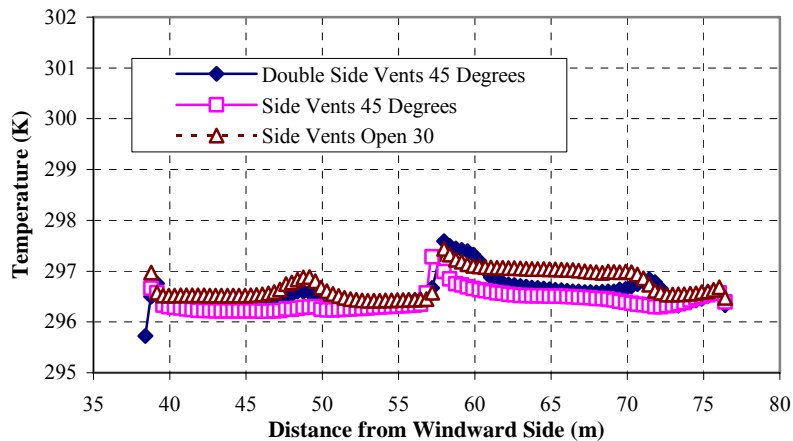


Figure 13: Temperature distributions for all three configurations (Roof Vents Open Windward)

From Figure 13 it should be clear that opening the side vents only 30° rises the temperatures inside both the west and east spans slightly more compared to the other two cases. Adding another row of ventilators yields more efficient ventilation compared to a 30 degree opening, as the temperature drops slightly in both spans. If the ventilators are opened at an angle of 45°, the lowest overall temperature distribution occurs in both west and east spans. The overall temperature rise (approximately 1°C) over the central plastic partition for the windward cases is however lower compared to the temperature rise (between 2°C and 4°C) for the leeward cases.

As a last comment, the results for the 45 degree angle where the roof vents were opened toward the windward side, can be compared with a similar simulation Bartzanas (tunnel greenhouse) with side vents and no roof vents, and curved roof greenhouse, where the maximum normalized velocity is 0.56, which seems to compare reasonably with the current calculated value in the same region which is approximately 0.5 m/s.

CONCLUSION

The influence of various ventilator configurations on the indoor climate of a four span greenhouse was numerically analyzed by utilizing a CFD model. From the six simulations presented it is evident that the solutions are definitely time dependant, and that the indoor climate of the greenhouse is significantly influenced by three parameters, namely a combination of roof vents, side vents, and the number of rows of side vents.

Considering the opening angle of the side ventilators, if the roof vents are opened towards the leeward side, the entrance velocity for the 45° is slightly higher (approximately 0.1 m/s) compared to the 30° openings, while the velocity distribution is quite similar for the rest of the greenhouse for the two opening angles. Orienting the roof ventilators toward the windward side causes the flow to enter the greenhouse at a higher velocity (almost 0.4 m/s) for the 45° opening than the 30° opening. It seems that the angle of the side ventilator openings doesn't have as significant an effect on the indoor climate, but it does influence the velocity distribution at plant level noticeably if combined with a windward open roof ventilator, especially in the east compartments.

The results seem to indicate that by adding a second row of side ventilators together with a leeward facing roof ventilator, the indoor temperature at plant level is somewhat reduced (about 1°C in the west spans, and 2°C in the in the east spans.) compared to the case of only a single row of ventilators. For this case the velocity distribution in the west spans is slightly higher in the second compartment, but it doesn't seem to affect the flow in the east spans appreciably, as there is still little air movement. Combining a second row of side ventilators with a windward roof vent doesn't appear to influence the climate at plant level too significantly in the west spans, but the velocities and temperatures are influenced to some extent in the east spans.

The results obtained from these simulations indicate that vent arrangement and the number of vents have an appreciable influence on the indoor climate. It is also shown that CFD can be a useful tool in developing and designing greenhouse for optimum production. Future research will include investigating the effect of winds at low velocities on the ventilation, in order to amplify the influence of natural convection. The effect of radiation will also be implemented in the CFD models; an attempt will also be made to analyze the models in three dimensions.

ACKNOWLEDGEMENTS

The authors would like to express their gratitude to Dr. M van Staden and Mr. J. Cloete from Aerotherm in South Africa for providing the necessary resources and assistance to complete the simulations.

NOMENCLATURE

\bar{a}	face area vector	ρ	density
\bar{g}	gravitational vector	ϕ	scalar quantity
G	grid flux computed from mesh motion	Γ	diffusion coefficient
f_g	body force due to gravity		
\bar{v}	velocity		For units refer to the StarCCM+ documentation (2006)
\bar{v}_g	grid velocity		
S_ϕ	source term		
T_{ref}	operating temperature		
β	Coefficient of Bulk Expansion		

Subscripts and Superscripts

0	cell number
f	face quantity
V	cell volume

REFERENCES

- American Society of Heating, Refrigeration and Air-conditioning Engineers, (2001) 2003 *ASHRAE HVAC Applications SI Edition*, ASHRAE, Atlanta
- Bartzanas T., Boulard T., Kittas C., 2004, Effect of Vent Arrangement on Windward Ventilation of a Tunnel Greenhouse, *Biosystems Engineering*, Vol 88, pp 479-490
- Boodley J.W. (1981) *The Commercial Greenhouse*, New York: Delmar Publishers
- Boulard T., Haxaire R., Lamrani M.A., Roy J.C., Jaffrin A., 1999, Characterization and Modelling of the Air Fluxes induced by Natural Ventilation in a Greenhouse, *Journal of Agricultural Engineering Research* Vol. 74, pp 135-144
- Boulard T., Wang S., Haxaire R., 2000, Mean and Turbulent air flows and microclimatic patterns in an empty greenhouse tunnel. *Agricultural and Forest Meteorology*, 100, pp 169 - 181
- Jones W.P., Launder B.E., 1971, The prediction of Laminarization with a Two-Equation Model of Turbulence, *International Journal of Heat and Mass Transfer* Vol. 15 pp 301 - 314
- Kitaya Y., Shibuya T., Yoshida M., Kiyota M., 2004, Effects of Air Velocity on Photosynthesis of plant canopies under elevated CO₂ levels in a Plant Culture System, *Advances in Space Research* Vol. 34, pp 1466-1469
- Kittas C., Bartzanas T., 2006, Greenhouse Microclimate and Dehumidification Effectiveness under different Ventilator Configurations, *Building and Environment*, Vol. 42, Issue 10, pp 3774-3784
- Kruger S., Pretorius L., 2007, The Effect of Internal Obstructions in Naturally Ventilated Greenhouse Applications, *Proc 5th Int Conference on Heat Transfer, Fluid Mechanics and Thermodynamics 2007*, Sun City, South Africa
- Mistriotis A., Arcidiacono C., Picuno P., Bot G.P.A., Scarascia-Mugnozza, 1997, Computational Analysis of Ventilation in Greenhouses at zero- and low-wind-speeds. *Agricultural and Forest Meteorology* Vol. 88m pp 121-135.
- Ould Khaoua S.A., Bournet P.E., Migeon C., Boulard T., Chassériaux G., 2006, Analysis of Greenhouse Ventilation Efficiency based on Computational Fluid Dynamics, *Biosystems Engineering*, Vol.95, pp 83-98
- Patankar S.V., 1980, *Numerical Heat Transfer and Fluid Flow*. Washington: Hemisphere
- StarCCM+ (2006) CFD Manuals, CD-Adapco
- Versteeg, H.K., and Malalasekera W., 2007 *An introduction to Computational Fluid Dynamics, The Finite Volume Method*, 2nd ed., Pearson Prentice Hall, England.